JOURNAL OF GEOPHYSICAL RESEARCH, VOL. 102, NO. D11, PAGES 12,957–12,969, JUNE 20, 1997

Accurate determination of total ozone using SBUV continuous spectral scan measurements

J. Joiner[1] and P. K. Bhartia

Laboratory for Atmospheres, NASA Goddard Space Flight Center, Greenbelt, Maryland

Abstract. Over the last 2 decades, satellite data have been used to monitor long-term global changes in stratospheric ozone. In order to measure relatively small ozone trends on timescales of the order of a decade, degradation of instrument components must be accounted for, and accurate interinstrument calibration must be maintained. In this paper, we have used a self-calibrating method to accurately retrieve total ozone from backscatter ultraviolet spectra in the wavelength range 310 to 340 nm. Using the information contained in this spectral region, we correct for time dependent and time-independent wavelength errors and calibration errors as well as radiative transfer modeling errors. We use continuous spectral scan data from the Nimbus 7 solar backscatter ultraviolet (SBUV) instrument to retrieve total ozone at latitudes between 40°S and 40°N over the time period 1979 to 1986. These total column ozone retrievals are used to independently validate retrievals from the both Nimbus 7 total ozone mapping spectrometer (TOMS) and SBUV in discrete mode. TOMS and SBUV in discrete mode have better temporal and spatial coverage than SBUV in continuous scan mode and are two of the primary instruments used to derive long-term global ozone trends. The time dependence of the difference between total ozone retrieved from SBUV continuous scan and that derived from TOMS and SBUV discrete mode is 0.6±0.3%/decade or less depending on latitude. The SBUV continuous scan radiances are modeled to an accuracy of ±0.3% (1σ). Unfortunately, an instrument problem terminated continuous scan mode observations after 1986 so that the later years of TOMS and SBUV discrete mode observations cannot be validated. The methods developed here may also be applied to other continuous spectral backscatter ultraviolet instruments in order to intercalibrate total ozone retrievals. This will be particularly important when temporal overlap of ozone monitoring instruments does not occur as in the case of the Nimbus 7 and Earth Probe TOMS instruments. In addition, the methods used here are applicable to ground-based spectral ultraviolet measurements.

Introduction

One of the important uses of satellite remote sensing data has been and continues to be monitoring the long-term behavior of ozone in the Earth's atmosphere. Many of the satellite-based instruments used for global trend studies were not originally designed to measure small changes in ozone over relatively long timescales. For these instruments, much effort has been expended to account for changes in the characteristics of a single instrument and to integrate data obtained with different instruments for the purpose of identifying ozone trends.

Satellite backscatter ultraviolet (buv) instruments, such as the total ozone mapping spectrometer (TOMS) and the solar backscatter ultraviolet (SBUV) spectrometer, have been used extensively to derived global ozone climatologies and trends [e.g., *Stolarski et al.*, 1992; *Gleason et al.*, 1993; *Hood et al.*, 1993; *Herman and McPeters*, 1993; *DeLuisi et al.*, 1994; *Hollandsworth et al.*, 1995; *McPeters et al.*, 1994; *Randel and Wu*, 1995]. Several techniques have been developed in order to account for changes in the electronic and optical components of buv instruments that occur slowly with time. First order corrections to account for optical component degradation can be made by examining buv solar irradiance measurements [*Cebula et al.*, 1988]. A more sophisticated approach, known as pair justification, requires that the total ozone measured with different pairs of wavelengths be consistent [*Herman et al.*, 1991]. More recently, all 13.5 years of Nimbus 7/TOMS day were reprocessed using the version 7 algorithm [*McPeters et al.*, 1996] in which the instrument degradation is assumed to be second-order polynomial functions of wavelength in

[1] Also at Hughes STX Corporation, Greenbelt, Maryland.

Paper number 97JD00902.

the 312-380 nm range. The time-dependent coefficients of these polynomials were derived using radiances measured in three long-wavelength channels of the instrument where the ozone absorption is weak and long-term behavior of the radiances is highly predictable using radiative transfer theory. *Hilsenrath et al.* [1995] have used the shuttle-borne SBUV/2 (SSBUV) to adjust the pre-launch calibration of the NOAA 11 SBUV/2 instrument and to account for time-dependent changes in the calibration due to optical and electronic component degradation during the time period 1989 to 1993.

Satellite data are routinely compared with ground-based and *in situ* observations (and vice versa) as a means of validation [e.g., *Labow and McPeters*, 1993; *Reinsel et al.*, 1994; *McPeters et al.*, 1996; *Miller et al.*, 1996; *Planet et al.*, 1996]. These comparisons are somewhat limited owing to the relatively poor spatial coverage of ground-based measurements. Large station-to-station variability in data quality, interinstrument differences, and differences in retrieval algorithms also make comparisons between ground and satellite-based ozone observations problematic.

In this paper, we describe a method to accurately retrieve total ozone utilizing radiances measured continuously over the spectral range from 310 to 340 nm. The use of a large number of spectral elements in this wavelength region provides for an accurate determination of wavelength errors, time-dependent and time-independent calibration errors, and radiative transfer errors. The method is self-calibrating in the same sense as the pair-justification technique of *Herman et al.* [1991]. However, more accurate results can be obtained here because we use a larger number of spectral elements. The method uses a physically based radiative transfer model to account for the effects of multiple scattering (Rayleigh and Raman) and clouds.

We apply the method to continuous scan mode data from the Nimbus 7 SBUV at latitudes between 40°S and 40°N. These data were obtained approximately one day per month from 1979 to 1986. This is the first time the full complement of spectral elements from SBUV continuous scan data has been used to retrieve total ozone and simultaneously account for calibration and other errors. The retrieved total ozone is compared with both Nimbus 7 TOMS and SBUV discrete mode total ozone measurements. TOMS and SBUV discrete mode data have been used to estimate trends in total ozone with linear multiple regression models [e.g., *Stolarski et al.*, 1992; *Reinsel et al.*, 1994; *Hollandsworth et al.*, 1995]. In the regression models, there are terms to account for a linear trend in ozone, the seasonal cycle, the quasi-biennial oscillation (QBO), and the solar cycle. Recently, reported trends in total ozone derived from both TOMS and SBUV discrete mode data are negative at all latitudes. The trends were statistically insignificant in the tropics (~1%/decade ±2% 2σ), but larger statistically significant negative trends of between 2 and 4%/decade were observed at latitudes between 20° and 40° in both hemispheres [*Hollandsworth et al.*, 1995]. Our SBUV continuous scan measurements will be used to independently validate these derived ozone trends from TOMS and SBUV discrete mode.

The following section briefly describes the SBUV instrument and its different operating modes as well as the TOMS instrument. The next section provides an explanation of the forward model that is used here to compute SBUV continuous scan radiances given an ozone profile and other parameters. This is followed by a description of the inverse model used to retrieve total ozone from SBUV continuous scan radiances. The retrieved total ozone is then compared with that from SBUV in discrete mode and TOMS. We follow with an error analysis and provide estimates of the uncertainties in the retrieved total ozone. Future applications of the methods used here are suggested in the last section.

Instruments

The SBUV instrument flew on the Nimbus 7 spacecraft, which was launched in late 1978, and is described in detail by *Heath et al.* [1975]. Follow-on versions of this instrument (SBUV/2) have flown on the NOAA polar-orbiting satellites NOAA 9 (launched December, 1984), NOAA 11 (launched September, 1988), and NOAA 14 (launched in December, 1994) [*Frederick et al.*, 1986; *Ahmad et al.*, 1994]. The SBUV is a nadir-viewing double monochromator with a field of view of 11.3° or approximately 200 km. The instrument measures the spectral radiance from Earth and employs a diffuser to measure the spectral solar irradiance with the same optical components as used in the Earth view. The quantity used to determine ozone is the ratio of the Earth spectral radiance to the incoming solar irradiance which we will refer to as normalized radiance. Changes in the instrument optics over time will cancel in this ratio. However, changes in the reflectivity of the solar diffuser will not cancel, and if not properly accounted for will cause a time-dependent error in retrieved ozone.

SBUV can operate in one of two modes. In the primary SBUV operating mode, called the step scan mode, the instrument scans 12 preselected wavelengths between 252 and 340 nm with a spectral resolution of 1.1 nm. Wavelengths between 310 and 340 nm are sensitive to total ozone as well as to cloud and surface reflectivity. The shorter wavelengths are sensitive to the altitude distribution of ozone between about 20 and 0.7 mbar. In the secondary operating mode, called the continuous scan mode, SBUV obtains continuous radiance measurements over the wavelength range from 160 to 400 nm with 0.2 nm spacing also at 1.1 nm spectral resolution [*Schlesinger et al.*, 1988]. This mode was operated approximately once per month between 1979 and 1987. In early 1987, the instrument developed a problem that resulted in a significant decline in data quality. Continuous scan mode data is not available after that time, but discrete mode data was taken for approximately three more years, and a method has been developed to account for most of the error introduced

by the malfunction [*Gleason and McPeters*, 1995]. Because of a faulty instrument design, continuous scan observations from the SBUV/2 instruments are much noisier than those from the Nimbus 7 SBUV. Moreover, the NOAA 14 SBUV/2 cannot collect continuous scan observations as a result of a grating drive problem.

Because the satellite field of view moves approximately 6 km/s, the SBUV instrument employs a separate collocated filter photometer to account for changes in cloud and surface reflectivity. The photometer is centered at 343 nm, a wavelength relatively insensitive to ozone absorption, and has a 3 nm full-width at half-maximum (FWHM) bandwidth. During each spectral scan over the wavelength range from 310 to 340 nm, five photometer measurements (corresponding to continuous scan wavelengths 305, 312, 317, 331, and 339 nm) were archived in the data set used here.

TOMS instruments have flown on several spacecraft including Nimbus 7 (November 1978 to May 1993), Meteor 3 (August 1991 to December 1994), Earth Probe (July 1996 to the present), and the Advanced Earth Observing System or ADEOS (September 1996 to the present). The TOMS instrument is similar to SBUV in discrete mode in that it makes measurements of the normalized radiance at six wavelengths between 312 and 380 nm with approximately the same spectral resolution. The shorter wavelengths are sensitive to total ozone as well as cloud and surface effects. A subset of the longer wavelengths (wavelengths differ between instruments) function in the same capacity as the SBUV photometer in that they are used to determine surface and cloud reflectivities. Unlike SBUV, radiances at the six wavelengths are measured nearly simultaneously (to within 200 ms). The instrument also differs from SBUV in that it scans ±51° from nadir, providing daily global coverage. The TOMS field of view is 3° or approximately 50 km at nadir.

Both TOMS and SBUV were calibrated before launch using National Institute of Standards and Technology (NIST) spectral irradiance sources [e.g., *Janz et al.*, 1996; *McPeters et al.*, 1996]. In the latest processing of TOMS data (version 7), small wavelength- and time-dependent corrections were applied to the TOMS radiances after launch. These corrections were of the order of 0.5%.

Forward Model

The forward model is used to compute normalized radiance given an ozone profile and cloud/surface parameters (pressure and reflectivity). The full information content of SBUV continuous scan data in the wavelength range 310-340 nm has not been previously exploited because accurate radiative transfer calculations to account for multiple scattering (Rayleigh and Raman) are computationally burdensome. Here we have used a radiative transfer model similar to that used in the version 7 processing of TOMS data [*McPeters et al.*, 1996]. A brief description is given below.

The nadir backscattered ultraviolet monochromatic radiance I_m (for unit incident solar flux) is given by

$$I_m(\mu_o, R_s, \Omega, P_s) = I_o(\mu_o, R_s = 0, \Omega, P_s) + \frac{R_s\, I_g(\mu_o, \Omega, P_s)\, \gamma(\Omega, P_s)}{1 - R_s S_b(\Omega, P_s)}, \quad (1)$$

adapted from *Dave* [1964] where I_o is the radiation backscattered by the atmosphere, R_s is the surface or cloud reflectivity, I_g is the sum of the direct and diffuse radiation reaching the surface, γ is the transmittance of the reflected radiation in the direction of the satellite, S_b is fraction of the reflected radiance scattered back to the surface by the atmosphere, μ_o is the cosine of the solar zenith angle θ, Ω is total ozone, and P_s is surface or cloud pressure. At each wavelength, the Rayleigh scattering coefficient and ozone absorption coefficient are specified. The Rayleigh scattering coefficients are taken from formalisms derived by *Bates* [1984]. The ozone absorption coefficients used here were taken from *Bass and Paur* [1984] and *Paur and Bass* [1984]. In the radiative transfer calculation, an ozone profile and a temperature profile are specified. The temperature profile is needed because ozone cross sections are weakly temperature dependent. The effect of Mie scattering from aerosols is modeled accurately using the concept of Lambert-equivalent reflectivity by changing R_s in (1) [*Bhartia et al.*, 1993].

Because the full radiative transfer calculation is computationally burdensome, we have used an interpolation scheme to accurately compute radiances as in the work of *McPeters et al.* [1996]. I_o, I_g, γ, and S_b were computed for 26 ozone profiles (6 low-, 10 middle-, and 10 high-latitude profiles), 10 solar zenith angles (θ = 0°, 30°, 45°, 60°, 70°, 77°, 81°, 84°, 86°, 88°), and 2 surface pressures (1000 and 400 mbar) at wavelengths between 300 and 340 nm with a spacing of 0.049 nm. The ozone profiles were derived using ozone sonde data and profiles from the stratospheric aerosol and gas experiment (SAGE) [*Chu et al.*, 1989]. These profiles span total ozone values between 125 and 575 DU in 50 DU increments. For each ozone profile, a climatological temperature profile is supplied. The SAGE and sonde data are used only to provide a profile shape for a given latitude and total ozone amount and therefore should not introduce any significant bias.

Radiances at the appropriate observing conditions are accurately computed by piecewise cubic interpolation of $\ln(I_m)$ against $\ln(\cos(\theta))$ and linear interpolation of $\ln(I_m)$ against total ozone and pressure. Errors due to interpolation are of the order of 0.1%. The normalized radiance at the observed wavelength and spectral resolution, $I(\lambda_o)$, is computed using

$$I(\lambda_o) = \frac{\int I_m(\lambda) F_m(\lambda) B(\lambda - \lambda_o) d\lambda}{\int F_m(\lambda) B(\lambda - \lambda_o) d\lambda}, \quad (2)$$

where $B(\lambda)$ is the instrument bandpass, and F_m is the monochromatic solar irradiance. For SBUV, $B(\lambda)$ is

modeled to good accuracy by a triangular slit function with a FWHM bandwidth of 1.13 nm [*Heath et al.*, 1975]. F_m was taken to be a solar spectrum measured with the SOLSTICE instrument at a spectral resolution of approximately 0.2 nm [*Rottman et al.*, 1993; *Woods et al.*, 1993].

Rotational-Raman scattering (RRS) is the primary source of the Ring effect [*Grainger and Ring*, 1962] and causes filling-in and depletion of solar Fraunhofer lines. RRS should be accounted for in the radiance calculation. We used the model of *Joiner et al.* [1994], that agreed well with observations, to compute RRS effects on radiances. In this model, the RRS effect between 310 and 340 nm varies slightly with θ, R_s, and P_s and is relatively independent of the ozone profile. We computed RRS effects for each of the 10 solar zenith angles and 2 pressures used above. The RRS effect for a given observation is obtained by interpolating the precomputed values linearly with pressure at the closest solar zenith angle. This calculation is more accurate than that used by *McPeters et al.* [1996], because the solar zenith angle dependence has been included. Figure 1 shows that RRS effects are of the order of 1% or less at the spectral resolution and wavelengths used here.

Inverse Model

The inverse model is used to determine the values of total ozone and other parameters that minimize the difference between observed radiances and those computed using the forward model. The observed radiance in the spectral region 310 to 340 nm depends on both total ozone and the reflectance of radiation from clouds and/or the Earth's surface. In early versions of total ozone retrieval algorithms used for both SBUV discrete mode and TOMS, it was assumed that reflectivity was independent of wavelength. In this case a pair of wavelengths can be used to retrieve total ozone, where one wavelength is more sensitive to ozone than the other. However, if the reflectivity has a wavelength dependence, an error in the retrieved total ozone will occur with the pair algorithm. Time-dependent errors will also occur with this algorithm if wavelength-dependent instrument degradation occurs over time and it is not properly accounted for. In addition, time-dependent wavelength-independent degradation can also produce time-dependent errors in retrieved total ozone. Wavelength-independent degradation, when not accounted for, will result in a wavelength-dependent reflectivity error that will in turn produce an error in the total ozone retrieval.

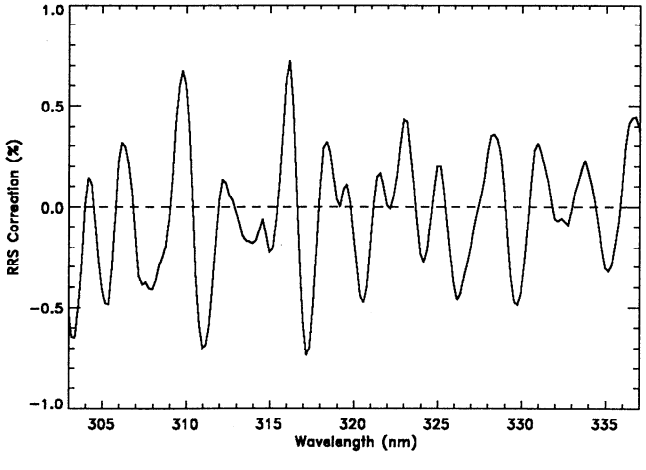

Figure 1. Percent change in radiance due to rotational-Raman scattering (RRS) computed for a scan with $\theta = 11°$ and cloud fraction $f \simeq 25\%$.

The version 7 TOMS retrieval utilizes a triplet of wavelengths to determine total ozone. The third wavelength is used to determine a component of reflectivity that is linear with wavelength [*McPeters et al.*, 1996]. This method alleviates some of the short-comings of the pair algorithm described above. Radiance residuals (differences between observed and computed radiances) at the long ozone-insensitive TOMS wavelengths are then used to correct for instrument degradation effects (both the time and wavelength dependence of radiometric errors) [*McPeters et al.*, 1996].

The general approach used here with data from SBUV continuous scan mode is similar to the TOMS triplet method. However, our approach differs from the triplet method in 2 important respects. First, we use 141 spectral elements from the SBUV continuous scan mode along with the monochromator as compared with the 3 spectral elements used in the TOMS triplet method. This allows for a more accurate determination of total ozone, reflectivity, and other parameters to account for calibration and forward model errors. Second, the wavelength range used here is much smaller than that of the TOMS triplet method (we use 310-340 nm here as compared with the 312-380 nm wavelength interval of the TOMS triplet method). The use of a smaller wavelength range minimizes errors resulting from radiometric errors with a nonlinear wavelength dependence.

Our retrieval method involves four steps: (1) Correct for wavelength errors (both scan-to-scan jitter and long-term drift). (2) Obtain an initial linearization point using the photometer to account for cloud/surface effects and a pair of wavelengths to obtain an initial guess for total ozone. (3) Adjust total ozone and other parameters to minimize the difference between observed and computed radiances using an iterative approach with 141 spectral elements between 310 and 340 nm. (4) Apply a time-dependent correction to the total ozone retrieved in step (3) to correct for calibration errors not detected in step (3) by utilizing the time dependence of the radiance residuals. The four step approach is necessary to maintain high accuracy for individual retrievals as well as to account for long-term drift in the instrument calibration. The details of each step will be described next.

Corrections to Instrument Wavelength

Before total ozone is determined from the observations, we account for two types of wavelength error: (1) scan-to-scan or short-term jitter in the wavelength scale and (2) long-term drift in the wavelength scale. Wavelength jitter manifests itself as a wavelength shift between individual radiance scans and the daily solar irradiance spectral scan. *Joiner et al.* [1995] showed that wavelength shifts between radiance and irradiance scans of the order of 0.01 nm can produce what appear to be much larger wavelength shifts (of the order of 0.1 nm) between observed and computed normalized radiance spectra. This apparent wavelength shift enhancement occurs because the RRS filling-in effect depends on the solar Fraunhofer line structure. Following *Joiner et al.* [1995], for each individual scan we determined the wavelength shift between the radiance and irradiance spectra that produced the highest correlation between the observed and computed RRS spectra. The wavelength shifts varied slightly from scan to scan. For example, the wavelength shifts between radiance and irradiance scans averaged 0.007 nm with a standard deviation of 0.01 nm and drifted slightly over time at a rate of approximately 0.001 nm/y. A close examination of individual scans also revealed that the wavelengths jitter slightly within a scan. This is probably the result of lack of a feedback mechanism to keep the wavelength cam rotating at a steady rate. This problem was corrected in SBUV/2 instruments. We did not attempt to correct for this effect as it did not significantly impact the retrievals.

In addition to the wavelength jitter, we also had to account for small wavelength differences between the observed and computed radiances. We can detect these small wavelength differences by making use of the sinusoidal (i.e., high frequency) component of the Huggins ozone absorption band. To isolate this component in the observed and computed normalized radiance spectra, we use a high-pass filter (HPF). The high-pass filter consists of convolving the spectra twice with a boxcar function of width approximately 4 nm. We determine a wavelength shift (to be applied to the observed radiances) that maximizes the correlation between the HPF observed and computed normalized radiance spectra. The wavelength differences between observed and computed spectra at the beginning of the observing period were determined to be of the order of a few hundredths of a nanometer. This difference is within the estimated wavelength uncertainty of laboratory spectroscopic measurements (R. D. Hudson, unpublished manuscript, 1992 summarized in the work of *Komhyr et al.* [1993]). The wavelength scale of the observations drifted slowly with time at a rate of approximately 0.0025 nm/y. This observed time dependence is consistent with that derived independently from a more accurate method utilizing SBUV solar irradiance measurements [*Cebula et al.*, 1988]. *Cebula et al.* [1988] noted that the magnitude of the wavelength drift increased slightly with decreasing wavelength. We did not attempt to account for the wavelength dependence of the wavelength drift as it had a negligible impact on the retrievals.

Initial Linearization

The SBUV measured radiances are non-linear functions of total ozone and cloud amounts. Since the instrument takes 14 s to scan the wavelength region 310-340 nm during which time the instantaneous field of view moves by 84 km owing to satellite motion, the cloud amounts typically vary with the wavelength position within the scan. To account for these effects, we make a first guess estimate of total ozone and correct the radiances for the motion of the satellite. The procedure is similar to that used for the discrete mode SBUV [*Fleig et al.*, 1990] but includes modifications developed for the TOMS V7 algorithm [*McPeters et al.*, 1996]. As in the discrete mode SBUV, we use collocated photometer measurements to correct for scene changes and derive total ozone using a pair of wavelengths (312/331 nm). However, unlike the discrete mode SBUV algorithm, we use the improved partial cloud correction scheme and better cloud height climatology developed for the TOMS V7 algorithm. We note that the cloud height climatology, derived from the international satellite cloud climatology project (ISCCP) [*Rossow and Schiffer*, 1988], may be in error by as much as 300 mbar or more [*Joiner and Bhartia*, 1995] on a scan-to-scan basis resulting in total ozone errors of up to 3%. These errors should be approximately the same for both the TOMS version 7 and our SBUV retrieved ozone.

Full-Spectral Three-Parameter Retrieval

Following corrections to the wavelength scale and using the initial guess specified in the linearization step, we adjust the total column ozone and two additional parameters in order to minimize the difference between observed and computed radiances. Using an iterative least squares approach (where all spectral elements are given equal weight) we solve for the three parameters in the following equation:

$$\ln I_{\mathrm{obs}}(\lambda) - \ln I_{n-1}(\lambda, \Omega_{n-1}) = a + b(\lambda - \lambda_o) + \Delta\Omega_n \left.\frac{\partial \ln I(\lambda)}{\partial \Omega}\right|_{\Omega=\Omega_{n-1}}, \quad (3)$$

where $I_{\mathrm{obs}}(\lambda)$ is the measured normalized radiance, $I_{n-1}(\lambda)$ and $\partial \ln I(\lambda)/\partial\Omega_{n-1}$ are the radiances and Jacobian, respectively, computed using the $n-1$ iteration estimate of total ozone Ω_{n-1}, a and b are coefficients to correct for radiometric or forward model error with a zero- and first-order wavelength dependence, respectively, $\Delta\Omega_n = \Omega_n - \Omega_{n-1}$, and $\lambda_o = 340$ nm. By solving for a and b in addition to $\Delta\Omega$, we accurately

account for systematic errors that have a constant or linear wavelength dependence. These types of systematic errors can occur as a result of diffuser degradation, error in the photomcter calibration, or a lincar wavelength dependence of the reflectivity. Because an initial linearization point was obtained in the previous step, the solution converges after only two iterations in every case. The left-hand side of (3) computed after the final iteration will be referred to as the residual. For small values of residuals it is nearly equal to the fractional difference between the observed and calculated radiances, i.e., $(I_{\text{obs}} - I_{\text{calculated}})/I_{\text{obs}}$.

Figure 2a shows radiances generated for three standard profiles at different latitudes, all with a total column ozone amount of 275 DU at a solar zenith angle of 0°. Figure 2b shows ratios of the spectra in Figure 2a to illustrate the profile sensitivity of the radiances. Ozone profile sensitivity is small for wavelengths longer than about 310 nm. As solar zenith angle increases, profile sensitivity begins at increasingly longer wavelengths. In this step, we use only wavelengths that are relatively insensitive to profile shape. A parameter referred to as slant ozone is used to determine the wavelengths used in (3), where slant ozone is defined as the product of normalized slant path and total ozone in DU divided by 1000 (i.e., $S\Omega = [1 + \sec(\theta_o)]\Omega/1000$ for nadir observations). For $S\Omega < 0.75$, we use wavelengths $310 < \lambda < 340$ nm, and for $0.75 < S\Omega < 1.5$ we use $315 < \lambda < 340$ nm. To limit profile sensitivity, we restricted our analysis to latitudes between 40°S and 40°N where $S\Omega$ is relatively small. Errors from profile effects are further reduced by using a low latitude profile at latitudes less than 30° and a midlatitude profile between 30° and 40° latitude. Figure 3 shows the Jacobians $(\partial \ln I/\partial\Omega)$ for the three standard profiles used above. The profile dependence of the Jacobian is relatively small and has a much smaller effect on retrieval accuracy than does the profile dependence of the forward model itself.

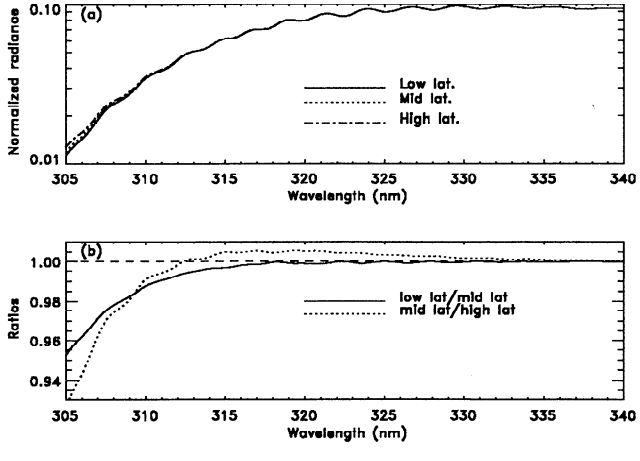

Figure 2. (a) Radiances computed using standard high-, low-, and mid-latitude profiles with total column ozone of 275 DU at $\theta = 0°$; (b) Ratio of radiances computed at low latitude to those computed at midlatitude for same profiles as used in Figure 2a and same ratio for middle- and high-latitude profiles.

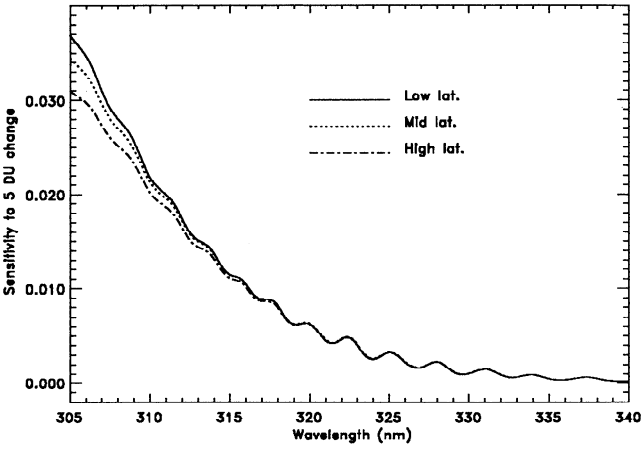

Figure 3. Jacobian or fractional change in radiance resulting from a 5 dobson unit (DU) change for same profiles as shown in Figure 2.

An examination of the magnitude and time dependence of the retrieved regression coefficients a and b reveals systematic errors (such as calibration drift) that have been accounted for in the retrieval algorithm. For example, b decreased linearly with time from about 0.02%/nm to -0.08%/nm from 1979 to late 1986. This linear time dependence is consistent with that expected as the result of diffuser degradation [e.g., *Cebula et al.*, 1988; *McPeters et al.*, 1996]. The value of b in late 1986 indicates that the normalized observed radiance at 310 nm is 2.4% too high relative to that at 340 nm. The average value of the constant term a was approximately 1% and the variation over time was relatively small (0.06%/y). The discrete mode and TOMS version 7 retrieval algorithms also attempt to account for these drifts [*Fleig et al.*, 1990; *McPeters et al.*, 1996] but cannot do so as accurately. Use of the full-spectral continuous scan data provides independent validation of these algorithms as will be discussed below.

We now show an example of the results obtained from this part of the algorithm for a single spectral scan. Figure 4 shows an example of observed and fitted normalized radiances. The difference between the two curves is not apparent in this figure. Figure 5 shows the residual or percent difference between the observed and computed radiances for the same scan (dotted line). The radiance increase of one order of magnitude over the wavelength range 305 to 335 nm is well modeled by the radiative transfer theory for this partially cloudy scene (derived cloud fraction ~25%). The standard deviation of the residual is 0.28%. Although some of the residual is the result of detector noise, scene noise, and other random processes, structure remains in the time-mean residual (average over all scans) as shown in Figure 5. This structure in the residual may result from several mechanisms that will be discussed later. The standard

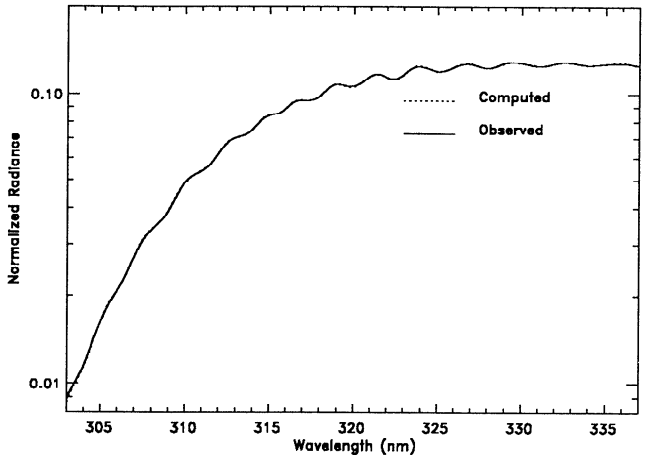

Figure 4. Observed normalized radiances for a scan taken on day 46 of 1979 at 2.1°S latitude with $\theta = 11°$ and normalized radiance computed after last iteration of retrieval.

deviation about the time-mean residual has an average value of approximately 0.3% which is consistent with that expected as a result of detector and scene noise. We also performed the retrieval using a wavelength-dependent error covariance (i.e., weighted least squares) with interwavelength correlation. However, this did not significantly reduce the variances or produce different results.

There is some evidence that the systematic component of the residuals may be the result of wavelength-dependent errors in the *Bass and Paur* [1984] ozone cross sections. Radiative transfer calculations show that the effect of such errors on the calculated SBUV radiances would be roughly proportional to $S\Omega$. We see indication of this dependence in our derived residuals. Our preliminary results show cross-section errors of approximately 1-2%. This is consistent with the uncertainty estimates made by R. D. Hudson (unpublished manuscript, 1992, reported in the work of *Kohmhyr et al.* [1993]) based on comparison of ozone absorption spectra measured by various laboratories. However, the ozone cross-section errors we derive would not explain all the structures that we see. We have also ruled out the possibility that an error in atmospheric temperature could produce the observed patterns in the residuals. Further investigation is required to better understand the small systematic component of the residuals.

Time-Dependent Correction Step

In the previous section in our regression model (3), we made the explicit assumption that the change in the SBUV-measured radiances with time resulting from diffuser degradation was linear with wavelength. In this section we examine the possibility that this may or may not have been the case.

We simulated the effects of a radiometric error with a quadratic wavelength dependence on the derived residuals. Figure 6 shows that the residuals have a low-frequency as well as a high-frequency component. The latter is highly correlated with HPF Jacobian. Although the size of this signal is small, it should be easily observable by examining long-term changes in the daily mean residuals, which vary little from day-to-day. We also note that examination of the time-dependent changes in the residuals would alert us to more complicated changes in the instrument calibration with wavelength.

Figure 7 shows that the daily mean residuals maintained their overall pattern throughout the lifetime of the instrument, indicating that the instrument did not develop anomalous behavior as function of wavelength. However, as Figure 8 shows, the magnitude of the residuals did change with time in a systematic way. Figure 9 shows that the linear trend has a wavelength dependence that is anti-correlated with the HPF Jacobian.

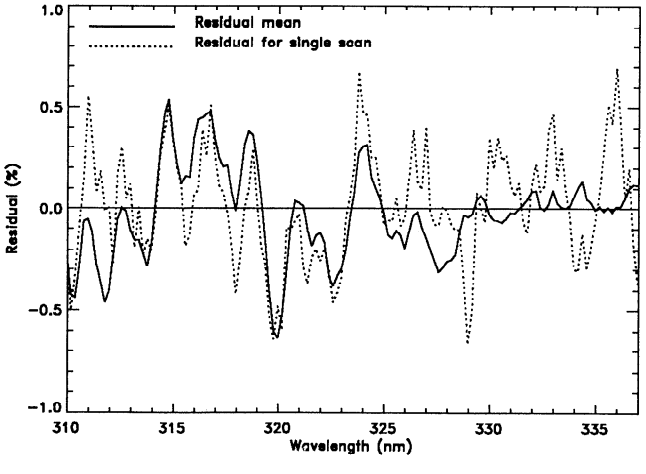

Figure 5. (Dotted line) Residual (percent difference between the observed and computed radiances) for scan used in Figure 4; (solid line) Average residual over all scans.

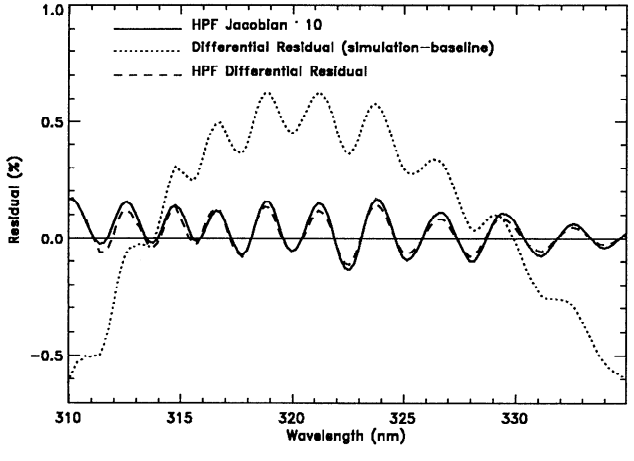

Figure 6. Differential residual (residual when simulated calibration error with quadratic wavelength dependence applied minus baseline residual) and HPF differential residual and Jacobian.

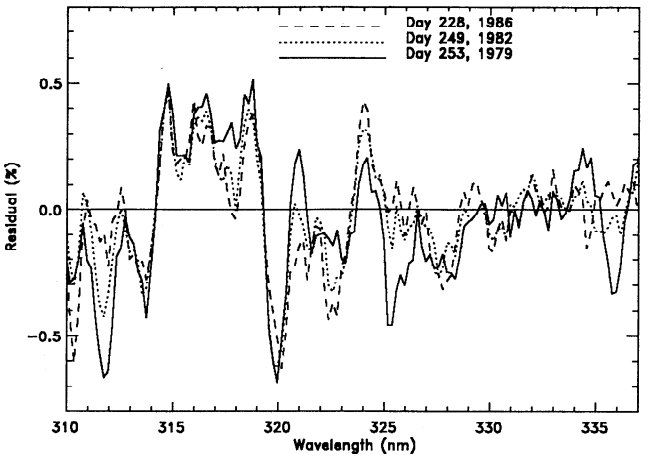

Figure 7. Daily mean residuals for three selected days.

On the basis of our simulation result shown in Figure 6, this indicates that the instrument calibration drift was not precisely linear in wavelength. By correlating the time-dependent component of the residual with the HPF Jacobian we estimate an error of -0.130±0.007%/y in the ozone results derived in the previous section. In our subsequent analysis we shall use this corrected data for comparison with TOMS and discrete mode SBUV.

One may wonder why we have chosen to do an off-line correction for the non-linear wavelength dependence, rather than including a quadratic term in our regression model (3). We found that the inclusion of a quadratic term in the regression model increases the retrieval error considerably. This is because the Jacobian has a strong quadratic term and the systematic component of the residuals (Figure 5) is much larger than that due to the quadratic term (Figure 7). Our off-line correction model provides more robust estimates of total ozone for a single scan, yet allows correction for small drifts not accounted for by the original model. It is also possible to retrieve total ozone with this step alone. This would be similar to the differential optical absorption spectroscopy (DOAS) approach that has been used for analyzing ground-based measurements [e.g., *Solomon et al.*, 1987] and is being used for preliminary total ozone retrievals with the global ozone monitoring experiment (GOME) instrument [*Eisinger et al.*, 1996]. Because of errors described above, we found that this method produced rather large random and systematic errors on a scan-to-scan basis. It remains to be seen whether these errors will be significant for a higher spectral resolution instrument such as GOME.

Results

The SBUV continuous scan retrievals can be used for trend studies. However, the spatial and temporal sampling is much poorer than that of either TOMS or the SBUV discrete mode. Alternatively, the continuous scan results can be used to independently validate TOMS and SBUV discrete mode measurements that are used for trend studies. The latter approach is used here.

Because discrete mode SBUV observations are made on different days than SBUV continuous scan mode observations, we cannot directly compare the results from the two operating modes. However, we can make comparisons on a zonal mean basis in the tropics where the day-to-day variability in the zonal mean total ozone is relatively small. Figure 10 shows a sample of retrieved daily zonal mean averages of total ozone between 20°S and 20°N from SBUV continuous scan mode and from SBUV discrete mode. The discrete mode daily zonal mean averages are shown by a continuous line for comparison. The total ozone derived from the SBUV discrete and continuous scan modes differed by an average of 2%. Therefore the continuous scan results have been multiplied by a constant value of 0.98 so that the two measurements can be more easily compared. The two types of retrievals produce similar seasonal variability although some systematic differences, such as in early 1982, are apparent. These discrepancies most likely result from sampling differences.

The zonal mean total ozone retrieved with SBUV continuous scan was an average of 2% higher than that from interpolated SBUV discrete mode. There are several possible explanations for this bias. The retrieval algorithms that produced total ozone from the continuous and discrete modes shown here differ in several respects including the way in which clouds effects are accounted for [*Fleig et al.*, 1990]. Accounting for radiometric and forward model errors with a linear wavelength dependence in the continuous scan retrievals and not doing so in the discrete mode retrievals explains some but not all of the systematic differences. The continuous scan mode minus interpolated discrete mode daily zonal mean total ozone had a relatively small time-dependence of 0.6±0.3%/decade (the uncertainties here and henceforth are all 1 σ) for the time period 1979-1987

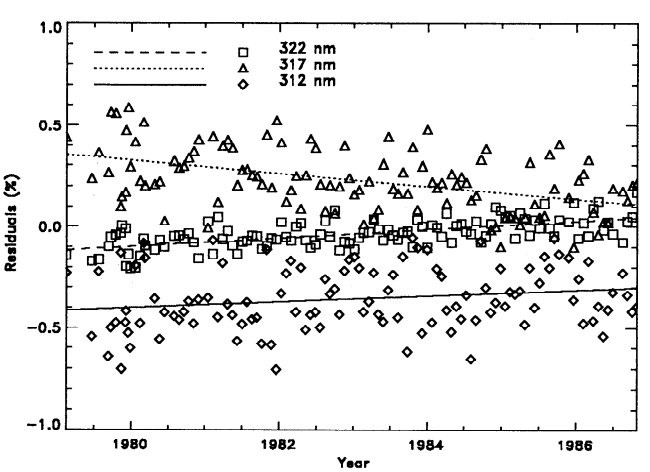

Figure 8. Time dependences of residuals at three wavelengths and linear fits. Each point represents the daily mean residual at a given wavelength.

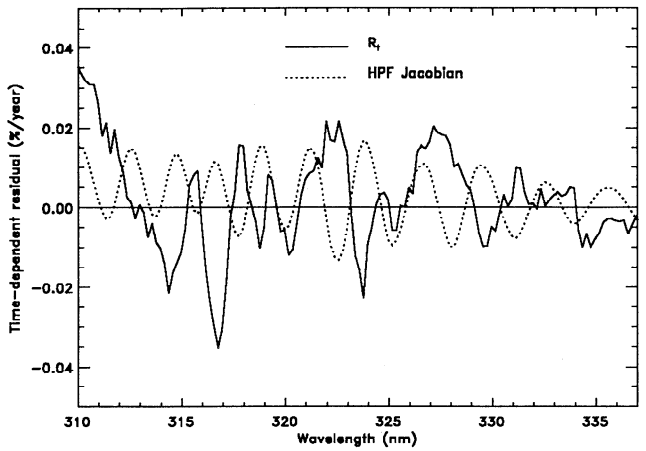

Figure 9. Linear time-dependent component of the residual, R_t, in %/y and HPF Jacobian.

(i.e., the SBUV continuous scan mode total ozone has a slightly smaller negative ozone trend at these latitudes than that from SBUV discrete mode).

In order to compare the total ozone derived from SBUV continuous scan with that from TOMS, individual TOMS spots were averaged over the area covered by the SBUV field of view during the time in which it scanned wavelengths from 310-340 nm. Approximately 15 TOMS spots covered the appropriate SBUV field of view. The TOMS and SBUV instruments compared here both flew on the Nimbus 7 satellite, so that the observations are perfectly collocated in time.

Figure 11 shows zonally averaged total ozone in the region 20°S to 20°N from the SBUV continuous scan and that from version 7 [*McPeters et al.*, 1996] collocated TOMS observations as a function of time. Again, the continuous scan results are multiplied by a constant (0.97) for comparison because of a 3% bias between total ozone from TOMS and SBUV continuous scan. The trend difference between the two measurements was 0.6% ± 0.3%/decade and is the same as the SBUV continuous scan and discrete mode trend difference at these latitudes. Figures 12 and 13 are similar to Figure 11 but show zonal averages between 20°N and 40°N, and 20°S and 40°S, respectively. The trend differences in Figures 12 and 13 were statistically insignificant (-0.1±0.3 and 0.05±0.3%/decade, respectively).

The structure of the agreement between SBUV continuous scan and TOMS is better than that between SBUV continuous scan and discrete modes. This is further evidence that the SBUV continuous/discrete mode discrepancies are the result of sampling differences. The sampling difference is removed in the SBUV continuous scan/TOMS comparison, because each SBUV continuous scan mode observation is paired with one collocated, averaged TOMS observation, and the zonal averaging is applied to the paired observations. The discrete/continuous mode SBUV data cannot be compared in the same way.

As in the SBUV continuous scan/discrete mode comparison, the SBUV continuous scan retrieved ozone is higher than that from TOMS by 2-3%. The mean TOMS/SBUV continuous scan total ozone difference has a dependence that is approximately quadratic with reflectivity. Total ozone differences were approximately 1% at high reflectivities and 4% at low reflectivities. This difference is most likely the result of a problem with the TOMS instrument. Smaller differences between TOMS and SBUV continuous scan retrieved total ozone (~0.5%) are dependent on latitude, $S\Omega$, and season. Comparison of ozone measured with SSBUV (with the most recent SSBUV calibration) and TOMS have shown that total ozone retrieved with SSBUV is about 2% higher than that from TOMS (E. Hilsenrath, private communication, 1996). This is consistent with our SBUV continuous scan results. The reflectivity de-

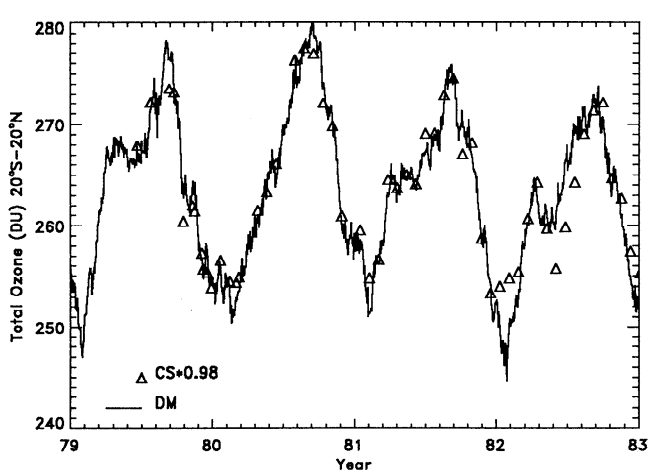

Figure 10. Daily zonal averages of total ozone between 20°S and 20°N retrieved with SBUV in continuous scan mode (CS) and in discrete mode (DM). The CS results are scaled by a factor of 0.98 to remove the 2% bias between CS and DM results.

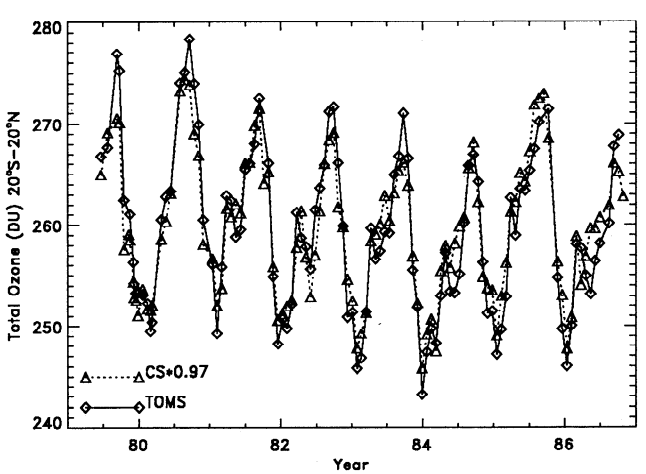

Figure 11. Daily zonal averages of total ozone between 20°S and 20°N retrieved with SBUV continuous scan mode (CS) and TOMS. The CS results are scaled by a factor of 0.97 to remove the 3% bias between CS and TOMS results.

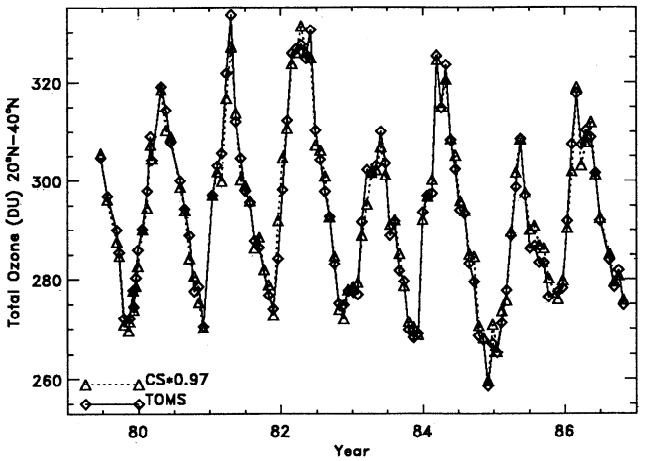

Figure 12. Same as Figure 11 but for latitudes between 20°N and 40°N.

pendence of the TOMS-SSBUV ozone difference was also consistent with the TOMS-SBUV continuous scan difference.

Another explanation for the interinstrument bias is that we have applied an absolute wavelength scale adjustment with respect to the laboratory measurements here that is not applied to TOMS or SBUV discrete mode. However, if this adjustment is not made, the interinstrument bias increases rather than decreases, and the increase is relatively small (less than 0.5%).

McPeters et al. [1996] compared TOMS version 7 retrieved total ozone with 30 ground-based stations (Dobson and Brewer instruments) at northern midlatitudes. The trend difference was 0.2%/decade which was within measurement uncertainty. TOMS was an average of 0.5% higher than the ground-based measurements. Therefore, the time-dependence of our SBUV continuous scan-retrieved total ozone is consistent with the trends derived from ground-based measurements. However, again the absolute value of our retrieved total ozone is approximately 3-4% higher than that from ground-based measurements. There are several possible explanations for this bias including algorithmic differences between the ground-based and SBUV continuous scan retrievals. At this time, the bias between total ozone from SBUV continuous scan, SBUV discrete mode, TOMS, and Dobson instruments remains an unresolved issue that is under investigation.

Error Analysis

A description of error sources in buv measurements is given by *McPeters et al.* [1996] and will be reviewed briefly below. In general, three types of error in retrieved total ozone are possible: (1) random or scan-to-scan error (2) time-invariant systematic errors which we will refer to as zero-point bias (3) time-dependent systematic errors. Random errors are produced by a combination of detector noise, scene change noise, errors in the atmospheric temperature, error in the assumed tropospheric ozone to which radiances are less sensitive [*Mateer et al.*, 1971], wavelength jitter, and retrieval error (including profile shape and cloud pressure error). Zero-point bias results from errors in the radiative transfer calculation including incorrect calculation of Rayleigh scattering, rotational-Raman scattering (e.g., bias in climatological cloud heights as discussed by *Joiner and Bhartia* [1995]), and the use of incorrect ozone cross sections or an incorrect climatological profile shape. Time-invariant wavelength errors, radiometric errors, and retrieval errors will also contribute to zero-point bias. Time-dependent systematic errors can result from time-dependent wavelength and radiometric errors as well as time-dependent changes in atmospheric conditions such as temperature, cloud pressures, and the ozone profile (especially tropospheric ozone). Volcanic SO_2 can also affect radiances in the wavelength region used here and can potentially produce time-dependent errors in retrieved total ozone. However this effect should be negligible as the scans with detectable amounts of SO_2 as described by *McPeters et al.* [1984] have been removed from the data set used here.

Error estimates are summarized in Table 1 and are described in detail below. One of the most important aspects of the approach used here with SBUV in continuous scan mode is that time-dependent calibration errors are significantly reduced as compared with TOMS and SBUV discrete mode. Several of the components of the total error budget (e.g., errors resulting from uncertainties in the ozone cross sections or tropospheric ozone) are identical for all buv-type instruments.

The radiance residuals can be used to estimate the magnitudes of the different types of error. In order to estimate the random component of the total ozone error, we remove the time-independent component of the residual (i.e., we use the variances about the time-mean residual as shown in Figure 5). Propagating the

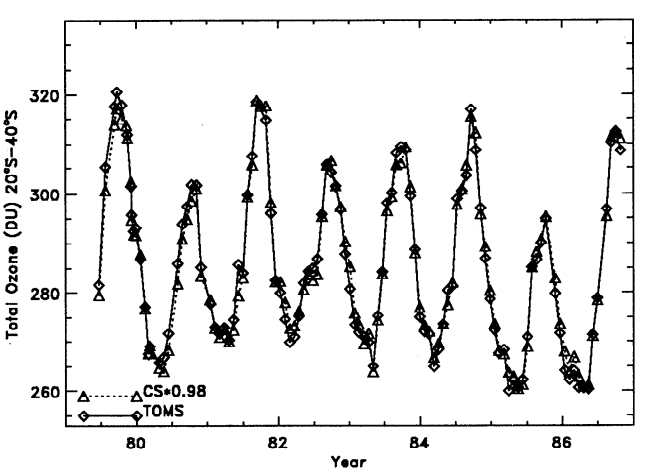

Figure 13. Same as Figure 11 but for latitudes between 20°S and 40°S. The CS results are scaled by a factor of 0.98 to remove the 2% bias between CS and TOMS results.

Table 1. Error components for total ozone from SBUV continuous scan

Source		Error(%)
Random		
	Instrument noise, scene change noise, λ jitter	0.15
	Cloud pressure, temperature, trop. O_3, profile shape	2.0
Zero-point bias		
	Radiometric, wavelength calibration, retrieval error, etc.	0.5
	Absolute error in O_3 cross-sections	2.5
Time-dependent		
	Radiometric and wavelength calibration	0.15/decade
	Atmospheric temperature	0.5/decade
	Tropospheric ozone	0.05/% change

variances through the retrieval process [e.g., *Rodgers*, 1990] and assuming that the radiance errors are not correlated between wavelengths, we estimate the random error in retrieved total ozone to be approximately ~0.15%. This estimate does not include the components due to errors in cloud pressure, atmospheric temperature, profile shape, or tropospheric ozone, which total approximately 2%.

To estimate the magnitude of the zero-point bias, we use the mean residual, account for interwavelength correlation, and propagate the error covariance as described above. The estimated uncertainty in the absolute value of retrieved total ozone using this approach is approximately ~0.5%. This estimated uncertainty is consistent with that obtained using a jackknife approach [*Miller*, 1974] in which blocks of 5 radiance observations are dropped and the retrieval is recalculated [*L. Flynn*, private communication]. This uncertainty is smaller than that reported for other buv observations. The observed interinstrument differences are within the uncertainties of the measurements, because TOMS and SBUV discrete mode have higher uncertainties in the absolute calibration. We have not included the 2.5% absolute uncertainty in the ozone cross sections here in our estimate of zero-point bias.

The uncertainty in the time-dependence of the retrieved ozone was estimated above to be of the order of 0.1% per decade based on a regression analysis in which a number of assumptions were made. The main assumption made was that the time dependence of the residual was due to a radiometric error and not to an atmospheric effect such as a temperature trend. The lower stratospheric temperature trends deduced from satellite data at the latitudes and time period examined here are reported to be statistically insignificant [e.g., *Randel and Cobb*, 1994]. We performed a multiple regression as in step (4) to include the potential effect of a temperature trend. In this test, we obtained a statistically insignificant temperature trend, but the ozone trend changed by 0.5%/decade. We will therefore take 0.5%/decade to be the upper limit on the trend uncertainty. The uncertainty due to changes in tropospheric ozone has been given by *McPeters et al.* [1996].

Although we have not utilized wavelengths shorter than 310 nm in the retrieval, we examined both the stationary and nonstationary components of the residuals at wavelengths between 305 and 310 nm as a consistency check. The treatment of these spectral elements is not complete, because profile shape effects have not been fully accounted for. However, examination of the residuals at these wavelengths provides some additional confidence in our results. At 305 nm, the stationary component of the error was approximately -1.5% which can be considered as an upper limit for zero-point bias. The time-varying component of the residual at 305 nm after the four step retrieval is ~0.05%/y or 0.5%/decade. This is consistent with the previously derived upper limit for the trend error.

Conclusions and Future Work

It has been shown that continuous spectral scan buv measurements are extremely valuable because they can be used (1) to accurately determine total ozone on a scan-by-scan basis (2) to accurately account for calibration (radiometric and wavelength) drift over time and (3) to validate long-term trends in total ozone derived from other instruments with higher temporal and spatial resolution but fewer spectral elements. The total ozone retrievals obtained here from SBUV continuous scan measurements have independently verified previously reported negative trends in total ozone obtained with TOMS and SBUV in discrete mode. The methods developed here can be applied to ground-based instruments as well as to SBUV/2 instruments that fly routinely on NOAA operational satellites. It is hoped that problems with the continuous scan mode on SBUV/2 instruments will be fixed so that the rich information content of these measurements can be fully utilized.

Another important application of the method used here is that it can be used for intercalibration of buv instruments. Intercalibration will be particularly important for instruments with discontinuous temporal coverage such as the Nimbus 7 TOMS which operated from 1979 to mid-1993 and Earth Probe TOMS, which was launched in July 1996. For accurate intercalibration, we must be able to separate instrument-dependent and -independent components of the mean radiance residual. An opportunity to do this arises with the high resolution spectral data collected by the

European Space Agency's GOME instrument [*Global Ozone Monitoring Experiment Interim Science Report*, 1993]. Because SBUV and GOME measurements are based on a completely different instrument design, it should be possible to separate instrument-independent and instrument-dependent errors. Future work will also include evaluating potential sources of error, including those due to calibration and the retrieval algorithms, that would produce biases between SBUV continuous scan, TOMS, SBUV discrete mode, and ground-based total ozone retrievals. Finally, the methods used here can be extended to higher latitudes and shorter wavelengths if profile shape effects are accounted for.

Acknowledgments. The authors would like to thank L. Flynn, E. Hilsenrath, J. Gleason, O. Torres, R. McPeters, and D. Larko for helpful discussions and assistance with TOMS and SBUV data and D. Richardson for providing the radiative transfer tables. The authors also wish to thank two anonymous reviewers for helpful comments. This work was supported in part by NASA grant NAS5-31755.

References

Ahmad, Z., M. T. DeLand, R. P. Cebula, H. Weiss, C. G. Wellemeyer, W. G. Planet, J. H. Lienesch, H. D. Bowman, A. J. Miller, and R. M. Nagatani, Accuracy of total ozone retrieval from NOAA SBUV/2 measurements: Impact of instrument performance, *J. Geophys. Res.*, *99*, 22,975-22,984, 1994.

Bass, A. M., and R. J. Paur, The ultraviolet cross-sections of ozone, I, The measurements, in *Atmospheric Ozone*, edited by C. S. Zerefos and A. Ghazi, pp. 606-610, D. Reidel, Norwell, Mass., 1984.

Bates, D. R., Rayleigh scattering by air, *Planet. Space Sci.*, *32*, 785-790, 1984.

Bhartia, P. K., J. Herman, R. D. McPeters, and O. Torres, Effect of Mount Pinatubo aerosols on total ozone measurements from backscatter ultraviolet (BUV) experiments, *J. Geophys. Res.*, *98*, 18,547-18,554, 1993.

Cebula, R. P., H. Park, and D. F. Heath, Characterization of the Nimbus-7 SBUV radiometer for the long-term monitoring of stratospheric ozone, *J. Atmos. Oceanic Technol.*, *5*, 215-227, 1988.

Chu, W. P., M. P. McCormick, J. Lenoble, C. Brogniez, and P. Pruvost, SAGE II inversion algorithm, *J. Geophys. Res.*, *94*, 8339-8351, 1989.

Dave, J. V., Meaning of successive iteration of the auxiliary equation in the theory of radiative transfer. *Astrophys. J.*, *140*, 1292-1303, 1964.

DeLuisi, J. J., C. L. Mateer, D. Theisen, P. K. Bhartia, D. Longenecker, and B. Chu, Northern middle-latitude ozone profile features and trends observed by SBUV and Umkehr, 1979-1990, *J. Geophys. Res.*, *99*, 18,901- 18,908, 1994.

Eisinger, M., A. Richter, J. P. Burrows, and A. Piters, Studies on DOAS ozone column retrieval from the UV and visible measurements of GOME, paper presented at *GOME Geophysical Validation Campaign Workshop Proceedings*, European Space Agency, Frascate, Italy, 1996.

Fleig, A. J., P. K. Bhartia, B. M. Schlesinger, R. P. Cebula, K. F. Klenk, S. L. Taylor, and D. F. Heath, Nimbus 7 solar backscatter ultraviolet (SBUV) ozone products user's guide, *NASA Ref. Publ., 1234*, 1990.

Frederick, J. E., R. P. Cebula, and D. F. Heath, Instrument characterization for the detection of long-term changes in stratospheric ozone: An analysis of the SBUV/2 radiometer, *J. Atmos. Oceanic. Technol., 3*, 472-480, 1986.

Gleason, J. F., et al., Record low global ozone in 1992, *Science, 260*, 523-526, 1993.

Gleason, J. F., and R. D. McPeters, Corrections to the Nimbus 7 solar backscatter ultraviolet data in the "nonsync" period (February 1987 to June 1990), *J. Geophys. Res.*, *100*, 16,873-16,877, 1995.

Global Ozone Monitoring Experiment: Interim science report, *Eur. Space Agency Spec. Publ., SP-1151*, 1993.

Grainger, J. F., and J. Ring, Anomalous Fraunhofer line profiles, *Nature, 193*, 762, 1962.

Heath, D. F., A. J. Kruger, H. A. Roeder, and B. D. Henderson, The solar backscatter ultraviolet and total ozone mapping spectrometer (SBUV/TOMS) for Nimbus G, *Opt. Eng., 14*, 323-331, 1975.

Herman, J. R., and R. D. McPeters, Ozone depletion at northern and southern latitudes derived from January 1979 to December 1991 total ozone mapping spectrometer data, *J. Geophys. Res.*, *98*, 12,783-12,793, 1993.

Herman, J. R., R. Hudson, R. D. McPeters, R. S. Stolarski, Z. Ahmad, X. Y. Gu, S. Taylor, and C. Wellemeyer, A new self-calibration method applied to TOMS/SBUV backscattered ultraviolet data to determine long-term global ozone change, *J. Geophys. Res.*, *96*, 7531-7545, 1991.

Hilsenrath, E., R. P. Cebula, M. T. DeLand, K. Laamann, S. Taylor, C. Wellemeyer, and P. K. Bhartia, Calibration of the NOAA 11 solar backscatter ultraviolet (SBUV/2) ozone data set from 1989 to 1993 using in-flight calibration data and SSBUV, *J. Geophys. Res.*, *100*, 1351-1366, 1995.

Hollandsworth, S. M., R. D. McPeters, L. E. Flynn, W. Planet, A. J. Miller, and S. Chandra, Ozone trends deduced from combined Nimbus 7 SBUV and NOAA 11 SBUV/2 data, *Geophys. Res. Lett.*, *22*, 905-908, 1995.

Hood, L. L., R. D. McPeters, J. P. McCormack, L. E. Flynn, S. M. Hollandsworth, and J. F. Gleason, Altitude Dependence of stratospheric ozone trends based on Nimbus 7 SBUV data, *Geophys. Res. Lett.*, *20*, 2667-2670, 1993.

Janz, S., E. Hilsenrath, D. F. Heath, and R. P. Cebula, Uncertainties in radiance calibrations of backscatter ultraviolet (buv) instruments, *Metrologia*, *32*, 637-641, 1996.

Joiner J., and P. K. Bhartia, The determination of cloud pressures from rotational-Raman scattering in satellite backscatter ultraviolet measurements, *J. Geophys. Res.*, *100*, 23,019-23,026, 1995.

Joiner J., P. K. Bhartia, R. P. Cebula, E. Hilsenrath, R. D. McPeters, and H. Park, Rotational-Raman scattering (Ring effect) in satellite backscatter ultraviolet measurements, *Appl. Opt.*, *34*, 4513-4525, 1995.

Komhyr, W. D., C. L. Mateer, and R. D. Hudson, Effective Bass-Paur 1985 ozone absorption coefficients for use with Dobson ozone spectrometers, *J. Geophys. Res.*, *98*, 20,451-20,465, 1993.

Labow, G., and R. D. McPeters, Comparison of ozone measured by TOMS with ozone measured by ground stations, in *Ozone Data for the World, vol. 34*, pp. 239-293, Atmos. Environ. Serv., Downsview, Ontario, 1993.

Mateer, C. L., D. F. Heath, and A. J. Krueger, Estimation of total ozone from satellite measurements of backscatter ultraviolet Earth radiance, *J. Atmos. Sci., 28*, 1307-1311, 1971.

McPeters, R. D., Climatology of nitric oxide in the upper stratosphere, mesosphere, and thermosphere: 1979 through 1986, *J. Geophys. Res.*, *94*, 3461-3472, 1989.

McPeters, R. D., D. F. Heath, and B. M. Schlesinger, Satellite observation of SO_2 from El Chicón: Identification and measurement, *Geophys. Res. Lett.*, *11*, 1203-1206, 1984.

McPeters, R. D., T. Miles, L. E. Flynn, C. G. Wellemeyer, and J. Zawodny, A comparison of SBUV and SAGE II

ozone profiles: implications for ozone trends. *J. Geophys. Res.*, *99*, 1994.

McPeters, R. D., et al., Nimbus-7 total ozone mapping spectrometer (TOMS) data products user's guide, *NASA Ref. Publ., 1384*, 1996.

Miller, A. J., et al., Comparisons of observed ozone trends and solar effects in the stratosphere through examination of ground-based Umkehr and combined solar backscattered ultraviolet (SBUV) and SBUV-2 satellite data, *J. Geophys. Res.*, *101*, 9017-9021, 1996.

Miller, R. G., The jackknife- A review, *Biometrika, 61*, 1, 1974.

Paur, R. J. and A. M. Bass, The ultraviolet cross-sections of ozone, II, Results and temperature dependence, in *Atmospheric Ozone*, edited by C. S. Zerefos and A. Ghazi, pp. 611-616, D. Reidel, Norwell, Mass., 1984.

Planet, W. G., A. J. Miller, J. J. DeLuisi, D. J. Hofmann, S. J. Oltmans, J. D. Wild, I. S. McDermid, R. D. McPeters, and B. J. Connor, Comparison of NOAA-11 SBUV/2 ozone vertical profiles with correlative measurements, *Geophys. Res. Lett.*, *23*, 293-296, 1996.

Randel, W. J., and J. B. Cobb, Coherent variations of monthly mean total ozone and lower stratospheric temperature *J. Geophys. Res.*, *99*, 5433-5447, 1994.

Randel, W. J., and F. Wu, TOMS total ozone trends in potential vorticity coordinates, *Geophys. Res. Lett.*, *22*, 683-686, 1995.

Reinsel, G. C., G. C. Tiao, D. J. Wuebbles, J. B. Kerr, A. J. Miller, R. M. Nagatani, L. Bishop, and L. H. Ying, Seasonal trend analysis of published ground-based and TOMS total ozone data through 1991, *J. Geophys. Res.*, *99*, 5449-5464, 1994.

Rodgers, C. D., Characterization and error analysis of profiles retrieved from remote sounding measurements, *J. Geophys. Res.*, *95*, 5587-5595, 1990.

Rossow, W. B., and R. A. Schiffer, ISCCP cloud data products, *Bull. Am. Meteorol. Soc.*, *72*, 2-20, 1991.

Rottman, G. J., T. N. Woods, and T. P. Sparn, Solar-stellar irradiance comparison experiment 1, 1, Instrument design and operation, *J. Geophys. Res.*, *98*, 10,667-10,677, 1993.

Schlesinger, B. M., R. P. Cebula, D. F. Heath, and A. J. Fleig, Nimbus 7 solar backscatter ultraviolet (SBUV) spectral scans solar irradiance and Earth radiance product user's guide, *NASA Ref. Publ., 1199*, 1988.

Solomon, S., A. L. Schmeltekopf, and R. W. Sanders, On the interpretation of zenith sky absorption measurements, *J. Geophys. Res.*, *92*, 8311-8319, 1987.

Stolarski, R., R. Bojkov, L. Bishop, C. Zerefos, J. Stachelin, and J. Zawodny, Measured trends in stratospheric ozone, *Science, 256*, 342-349, 1992.

Woods, T. N., G. J. Rottman, and G. J. Ucker, Solar-stellar irradiance comparison experiment 1, 2, Instrument calibrations, *J. Geophys. Res.*, *98*, 10,679-10,694, 1993.

J. Joiner, Laboratory for Atmospheres, NASA Goddard Space Flight Center, Code 910.3, Greenbelt, MD 20771. (e-mail:joiner@dao.gsfc.nasa.gov)

P. K. Bhartia, Laboratory for Atmospheres, NASA Goddard Space Flight Center, Code 916, Greenbelt, MD 20771. (e-mail:bhartia@chapman.gsfc.nasa.gov)

(Received October 4, 1996; revised March 10, 1997; accepted March 11, 1997.)